

Quantifying Joint Uncertainties for Hybrid System Vibration Testing

Nadim A. Bari^{1,4}, Manuel Serrano², Safwat M. Shenouda³, Stuart Taylor⁴, John Schultze⁴,
Garrison Flynn⁴

¹Department of Mechanical Engineering
University of Michigan
Ann Arbor, Michigan 48109

²Department of Aerospace & Mechanical Engineering
New Mexico State University
Las Cruces, NM 88003

³Department of Mechanical Engineering
North Carolina A&T State University
Greensboro, NC 27411

⁴Los Alamos National Laboratory
Los Alamos, NM 87545

Abstract

Controlled laboratory vibration testing has been the preferred method to experimentally quantify a system's governing dynamic response. However, dynamic testing of full-scale commercial structures in service environments can be an expensive and challenging endeavor to perform due to structural size and complexities. Hybrid substructuring is a method that involves performing tests on components of interest coupled with a numerical model simulating behavior of the primary system. The physical test and the numerical model are combined to represent the dynamic response of the complete system. Hybrid substructuring could also be implemented in the opposite fashion: the primary system as the physical substructure and a component of interest as the numerical substructure. Such an approach enables predictions of the dynamic response of a critical component when it cannot be directly measured during a system test. Within the numerical model uncertainties in the coupling of substructures can be accounted for through probabilistic model parameters. Using this approach, the effects of uncertainties in the component of interest and its interface to the primary system, such as those due to jointed connections, are captured. This paper aims to quantify a system's uncertainties by incorporating a suite of experimental data with inverse analysis to determine distributions of uncertain parameters, thus allowing a hybrid substructuring scheme to make statistically bounded predictions. The approach is demonstrated through an analysis of the bolted joints uncertainties in the Box and Removable Component test structure.

Keywords: Bolted Joints, Modal Analysis, Model Calibration, Uncertainty Quantification, Vibration Testing

INTRODUCTION

Determining the complete dynamic response of large-scale engineering systems is critical for assessing performance of complex systems in their real-world operating environments. However, performing full-scale testing is difficult due to size, weight, and cost. Accurate testing and qualification of a full system, as well as each of its components, becomes increasingly difficult with system complexity. Test scenarios meant to replicate real-world conditions are rarely ideal. Examples of common challenges in testing include (1) inability to instrument a component directly (2) variability in jointed connections coupling the component to its system (3) laboratory test configurations unable to represent complexity of true service environment. New methods to increase reliability, reduce uncertainty, and limit over testing are of great interest to the structural dynamics community. Herein, we seek to alleviate such physical constraints to the greatest extent possible by representing critical components as a numerical substructure coupled to a physical substructure of the larger system.

Rather than full-scale testing, the behavior of the complete structure is commonly inferred from test results obtained from experiments on a scaled model of the entire structure or testing of a critical component of the structure (Lee et al. 2007). One approach to characterizing a system's dynamic response is pseudo-dynamic testing (PsD), in which only a vital element of the entire structure (typically a complex, difficult to model component) is tested physically while the remainder of the structure is modeled numerically (Takanashi 1980, Takanasi 1975, Mahin 1989). With PsD methods, the physical element is excited statically under loading conditions and not by dynamic excitations, such as ground acceleration, which leads to several experimental inaccuracies.

Recent technological advances in signal processing have allowed for full-scale structural testing to be performed on components of interest, with the remainder of the structure being numerically modeled. Hybrid Substructuring (HS) is a recently developed technique to investigate the dynamic behavior of structural systems (Blakeborough et al. 2001, Chen and Rieles 2012). These advances have led to a new, innovative approach to computing displacement, velocity, and acceleration of components under dynamic excitation during experimental settings (Nakashima et al. 1992). This testing technique, referred to as Real-Time Hybrid Substructuring (RTHS), is widely used for performance evaluations of structural systems subjected to dynamic loading (Fernandois 2019). RTHS is similar to the PsD testing method; however, with RTHS, both physical and numerical substructure partitions are simultaneously integrated into a real-time loop while the physical structure is dynamically excited (Dermitzakis and Mahin 1985). Once the theoretical model is validated as an accurate mathematical representation of the structure, HS is typically the simplest method of the two to perform because no transfer system or real-time control loop algorithm is required.

Both HS and RTHS are methods that rely heavily on a numerical model of a substructure to represent the dynamic response of the complete system accurately. Consequently, these approaches permit for impacts of uncertainties in the system, such as those due to jointed connections, to be incorporated into the numerical substructure as probabilistic variables. This paper aims to quantify a system's uncertainties by incorporating experimental data with an optimization algorithm to find probabilistic values of uncertain parameters so that system uncertainty may be propagated into a hybrid substructuring scheme. The methodology will be demonstrated through an analysis of the bolted joints uncertainties in the Box and Removable Component (BARC) test structure.

EXPERIMENTAL PROCEDURE

Test Component

The Box Assembly with Removable Component (BARC) test structure, developed at Sandia National Laboratories and Kansas City National Security Campus for the Boundary Condition Round Robin Challenge (Soine et al. 2019), was used in this study. This structure was explicitly designed as a standard system for researchers to integrate into a testbed when designing environmental shock and vibration tests, focusing on the issue of uncertain boundary conditions (Skousen et al. 2017, Soine et al. 2019). The BARC consists of two substructures. The base substructure

is a cut box frame and the removable component is a beam, with the two substructures connected by two C-channels. The BARC substructures are aluminum 6061 and the C-channels are aluminum 6063. The cut box substructure is 3" (7.62 cm) wide and 6" (15.24 cm) tall with a top cut of 0.5" (1.27 cm) and thickness of 0.25" (0.635 cm). The removable component is 1" (2.54 cm) wide and 5" (12.7 cm) long with a thickness of .125" (0.3175 cm). C-clamps are 1" (2.54 cm) wide and 2" (5.08 cm) tall.

The BARC was assembled onto the shaker table using four button cap screws with its flat faces normal to the direction of motion. The four mounting screws were hand tightened until secure. Then they were tightened using a socket wrench. The C-channel brackets were attached to the box frame using 8 stainless steel socket cap screws, which were each torqued to 20 in-lbs (Rohe 2018). The beam was then attached using 2 hex bolts, which were each torqued to 50 in-lbs. Although the specified assembly configuration is asymmetric, the BARC was assembled symmetrically for the results presented in this paper, as illustrated in Figure 1.

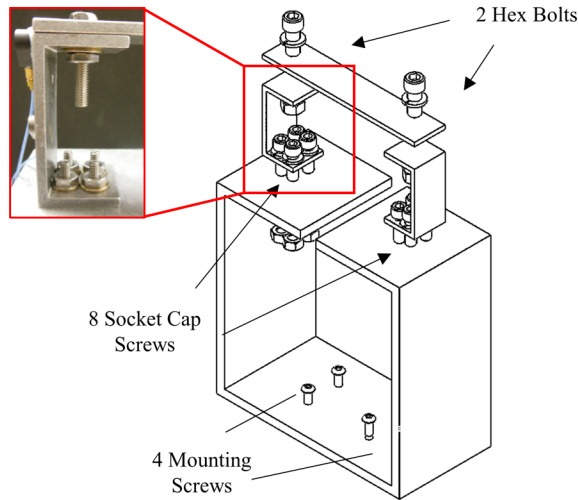


Figure 1: BARC structure in a symmetric test configuration with inset showing bolted connection of the box to the removable component.

Experimental Setup

The BARC was instrumented with eight single-axis accelerometers measuring along the axis of excitation, two on each leg of the box and two on each C-channel. A bi-axial accelerometer was placed at the center of the removable component measuring acceleration vertically as well as in the direction of excitation. Locations of the accelerometers are illustrated in Figure 2. Accelerometers were also placed at the base of the shaker table to measure the input acceleration and controlling the excitation. Due to hardware constraints the tests were run using two data acquisition systems with limited channels. Two sessions (referred to as session A and session B) were completed for every test to allow for data acquisition at all measurement locations. For each test, a random vibration with RMS of 0.005 g's was input as a base excitation for 30 seconds.

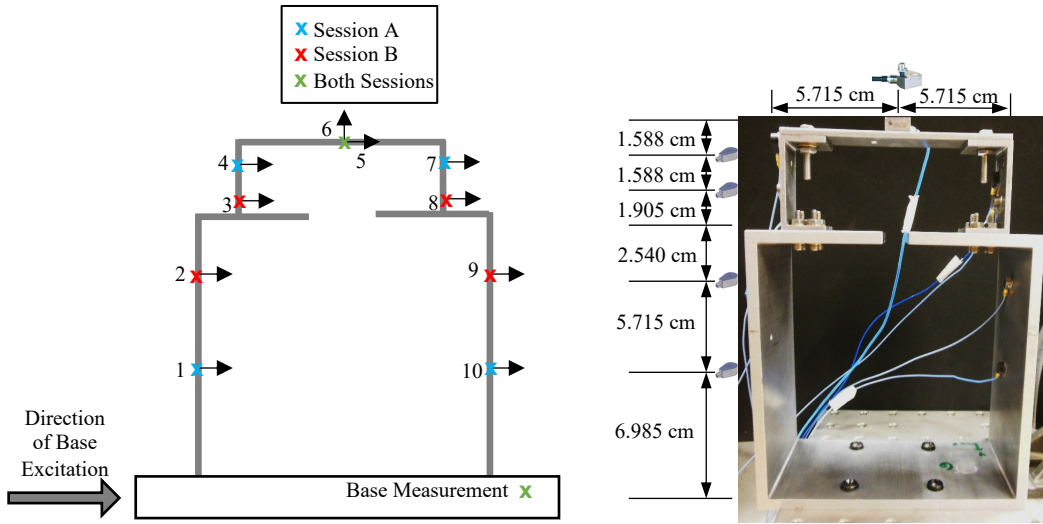


Figure 2: Acceleration measurement setup during BARC testing. A schematic for the accelerometer locations and node labels for test sessions A and B are shown on the left figure. Measurements at the top and base nodes were collected during both sessions. Uniaxial accelerometers measured acceleration in the direction of excitation symmetrically on the BARC vertical components and a bi-axial accelerometer measured vertical acceleration as well as acceleration in the direction of excitation on the top removable component.

Test Procedure

A total of 30 tests were completed where each test consisted of both sessions A and B. Between each test, the top two hex cap screws connecting the removable component to the C-clamps were loosened and then retorqued to 50 in-lbs. In addition to retorquing the top bolts, the 8 socket screws used to fasten the brackets to the box frame were also loosened and retorqued to 20 in-lbs.

NUMERICAL MODEL

The BARC system is modeled using Euler-Bernoulli beam elements. These elements exhibit three degrees of freedom at each node: axial, rotational, and translational. Because the BARC was assembled in a symmetric configuration for this paper, the out-of-plane dynamics of the BARC were assumed to be negligible. The BARC is modeled as a system containing nine beams, with each beam being modeled independently using finite elements. The local models are then appropriately coupled to form the global finite element model of the BARC.

Uncertainties in the numerical substructure would change the natural frequencies of the system. Thus only the natural response of the BARC was modeled as the natural frequency was used for validation. The equation of motion for the BARC is derived to be

$$[M]\ddot{\vec{y}} + [C]\dot{\vec{y}} + [K]\vec{y} = 0 \quad \text{Eq. 1}$$

where $[M]$ is the global consistent mass matrix, $[C]$ is the damping matrix, and $[K]$ is the global Euler-Bernoulli stiffness matrix. The global mass and stiffness matrices were derived from elemental mass and stiffness matrices (beam theory). The damping matrix was evaluated from a known modal damping matrix and was not experimentally determined (Farrar et al. 2016). The natural frequencies were evaluated as the square root of the eigenvalues of the mass and stiffness matrices.

These bolted joints are subject to self-loosening under vibrations; this may alter the natural frequencies of the system. Consequently, the uncertainties in the system come from the bolted joints. The bolted joints were modeled as single, massless, Euler-Bernoulli beam elements (springs). The three degrees of freedom at each node (axial, rotational, and translational) correspond to axial, rotational, and shear stiffness parameters. The BARC is modeled such that only the stiffness parameters of the bolted joints are associated with uncertainties of the system while all welded joints are assumed perfectly stiff. Figure 3 illustrates the location of the modeled spring elements.

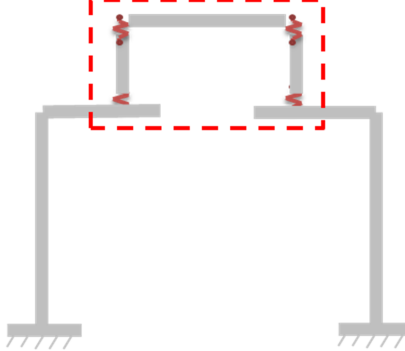


Figure 3: The BARC represented as an Euler-Bernoulli beam model with uncertain joint connections (highlighted in red) represented as spring elements.

ANALYSIS

Joint Stiffness Calibration

Parameters representing uncertainties present within the bolted joints of the removable component and the C-clamps were calibrated to each of the thirty tests (with bolts loosened and tightened between) independently, forming a distribution of calibrated joint stiffness values. These uncertainties were represented as varying axial, shear, and rotational stiffness values. The calibration was completed for each of the experimental repeats, producing a distribution of calibrated stiffness values.

Calibration of parameter values for each test seeks to minimize the root mean square difference between normalized natural frequency predictions, η , and normalized natural frequencies measured experimentally, y . Natural frequency predictions are normalized according to:

$$\eta = \frac{\omega_{exp} - \omega_{sim,i}}{(\omega_{exp} + \omega_{sim,i})/2} \quad \text{Eq. 2}$$

where ω_{exp} is the experimental natural frequencies and $\omega_{sim,i}$ is the predicted natural frequencies given the i^{th} parameter sample values. Experimentally measured natural frequencies are normalized according to:

$$y = \frac{\omega_{exp} - \omega_{sim,0}}{(\omega_{exp} + \omega_{sim,0})/2} \quad \text{Eq. 3}$$

where $\omega_{sim,0}$ is the model prediction with a set of nominal parameter values. Frequencies are normalized within the objective function so that all frequencies have equal weight rather than allowing high frequencies skewing the calibration.

5. Results and Discussion

Both HS and RTHS are methods that rely heavily on a numerical model of a substructure to represent the dynamic response of the complete system accurately. Consequently, these approaches permit for impacts of uncertainties, such as those due to jointed connections, to be represented numerically as probabilistic variables. Uncertainties in

the numerical substructure would change the natural frequencies of the system. Thus only the natural response of the BARC was modeled as the natural frequency was used for validation. This section presents the experimentally determined natural frequencies of the BARC with quantified uncertainties.

5.1 Experimentally Determined Natural Frequencies

The frequency response function (FRF) of the BARC was derived globally with respect to all measured degrees of freedom by combining acceleration output at each sensor location per acceleration input at the base of the structure. Figure 4 shows the global FRF for each of the thirty tests completed. The BARC is assumed to be a lightly damped system and a parameter-estimation method was used to determine the system's natural frequencies one mode at a time. Variability of the measured natural frequency resulting from the bolt uncertainty is illustrated in Figure 5. In this figure each of the first three modes is normalized by its nominal value such that we can see the test-to-test variation. Test set A includes measurements at degrees of freedom 1, 4, 5, 6, 7 and 10. Test set B includes measurements at degrees of freedom 2, 3, 5, 6, 8 and 9 (Figure 2).

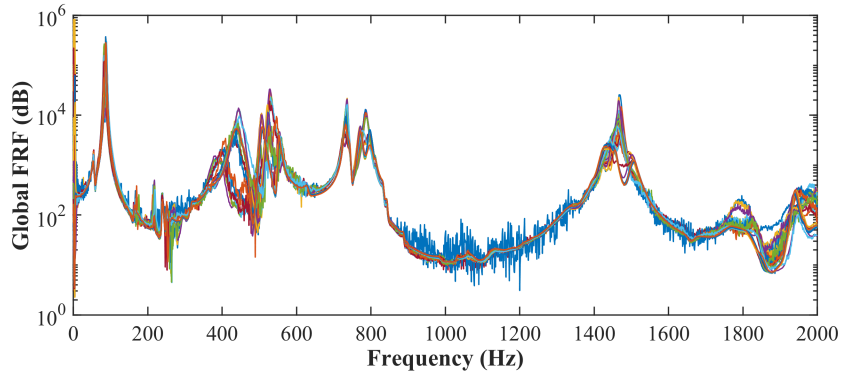


Figure 4: Transmissibility plots collected for thirty tests where the bolted joints were loosened and retorqued between each test.

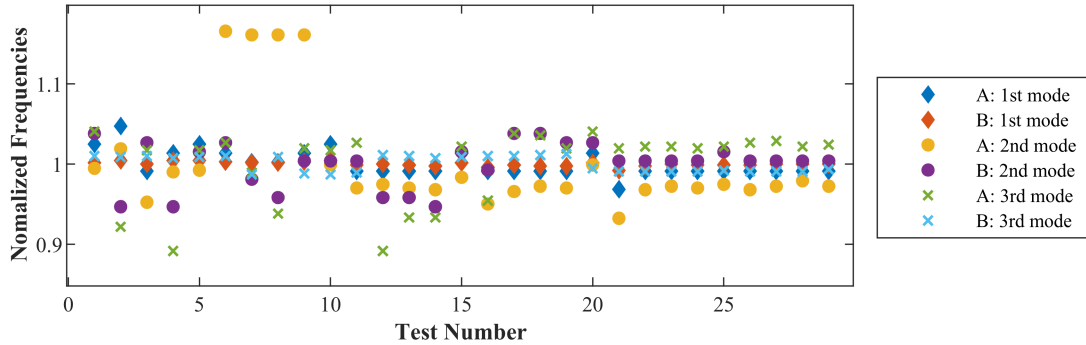


Figure 5: Variability in the first three experimentally measured natural frequencies due to joint uncertainty.

The simple mathematical model does not capture out of plane (torsional) motion. Therefore, more complex finite element model simulations were used to determine that the first four natural frequencies of the BARC which are correlated to in-plane mode shapes and any natural frequencies corresponding to torsional model shapes were removed from the analysis.

5.2 Stiffness Uncertainty Quantification

The optimization algorithm was developed to take in the experimental natural frequency values and output a distribution of stiffness values. Stiffness values are optimized such that the sum of squares residual of the

experimentally and numerically modeled natural frequencies are minimized. The univariate and bivariate distributions of the stiffness values, k_{axial} , k_{shear} , $k_{\text{rotational}}$, are shown in Figure 6 and statistics of the calibrated distributions are provided in Table 1. Correlations between the three stiffness parameters were not found to be statistically significant, which is a welcome observation to avoid trade-offs between the stiffness parameters.

Table 1: Statistics of calibrated stiffness parameters

Model Parameter	Minimum	Maximum	Mean	Std. Dev.
$k_{\text{axial}} (\text{N/m})$	1,000	10,796	5,861	3,016
$k_{\text{shear}} (\text{N/m})$	100	1,999	1,242	671
$k_{\text{rotational}} (\text{N/rad})$	25	199	112	58

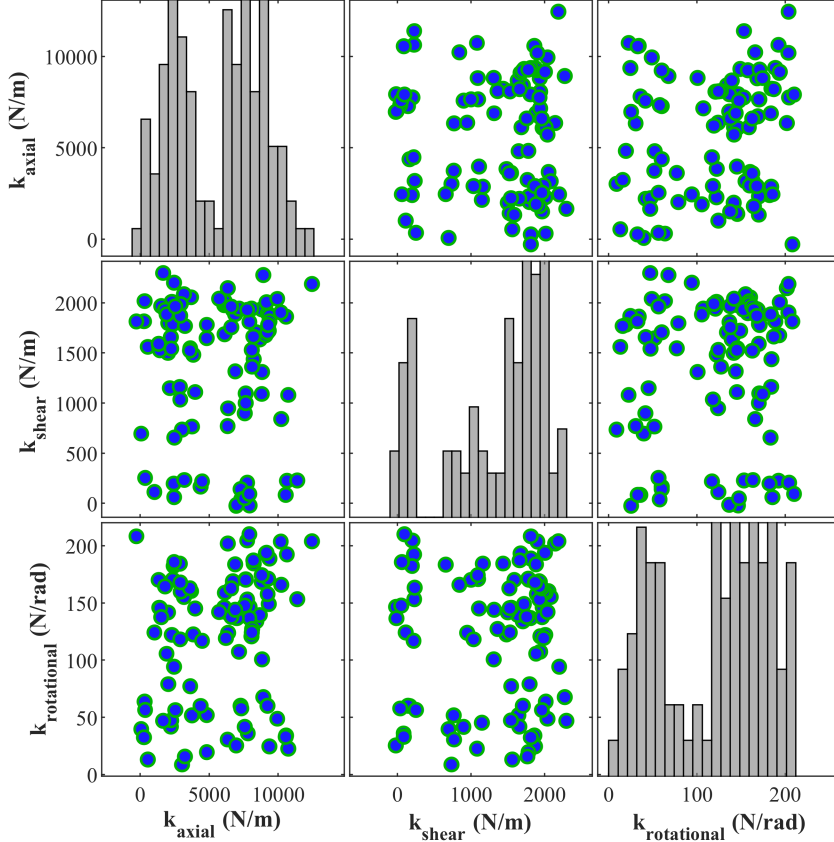


Figure 6: Distributions of the stiffness values. Along the diagonal are histogram plots of each stiffness values. The off-diagonal subplots of the matrix are scatter plots indicating the density of two independent stiffness values with respect to each other.

Distributions of the stiffness parameters are estimated using a kernel density estimate. Calibrated parameters distributions are then propagated forward to the numerical model to predict the BARC's first four natural frequencies corresponding to in-plane modes. Distributions of the predicted frequencies are shown in Figure 7 and summary statistics are provided in Table 2.

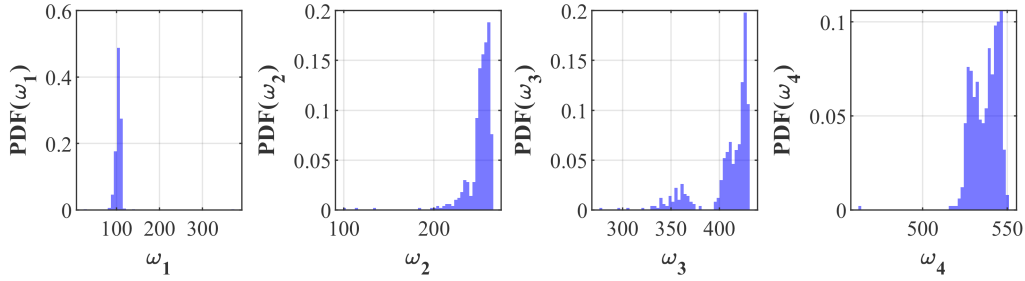


Figure 7: Distributions of the predicted frequencies given calibrated distributions of joint stiffness values.

Table 2: Statistics of forward model predictions considering joint uncertainty.

	Frequency Statistics (Hz)			
	Minimum	Maximum	Mean	Std. Dev.
Mode 1	27	372	105	13.7
Mode 2	102	266	251	15.6
Mode 3	278	431	408	26.7
Mode 4	462	551	537	8.19

CONCLUSIONS AND FUTURE WORK

This report investigates uncertainty in bolted joints by determining distributions of joint stiffness parameters with respect to experimentally captured variations in a structure's natural frequencies. Uncertainties in the system response were assumed to be related to the system's bolted connections (represented as stiffness parameters) which were loosened and tightened to the same torque between every test. Joint stiffness parameters were calibrated to every test independently resulting in a distribution of calibrated values. These calibrated values were then propagated forward in the numerical model to make new predictions of BARC frequencies with statistical bounds.

This paper served to demonstrate the ability to quantify and propagate uncertainties in a system that may be represented as substructures. The next step in this study is to incorporate the calibrated parameter distributions into a hybrid substructuring, and eventually real time hybrid substructuring, scheme. Simulations would be advanced to predict time series response, such as displacement, velocity, and acceleration with uncertainty bounds. Ultimately, the numerical model would be reduced to only the component and probabilistic joint parameters. Measurements could then be collected at the base of the joints and used as inputs to the numerical substructure, which in turn makes probabilistic predictions of the component. This substructured model would enable predictions of a component response after a full system test where the component could not be directly measured. Similarly, such a substructured model could be used to control a system vibration test in a scenario where the component is not accessible for instrumentation, presenting new opportunities for system qualification.

Finally, implementation of the methodology with a more complex model capable of predicting out-of-plane and torsional modes should be completed. Quantification of uncertainties with more advanced systems, such as a nonsymmetrical BARC are necessary to determine limitations of the method due to system complexities.

REFERENCES

- A. Blakeborough, M. S. Williams, A. P. Darby and D. M. Williams, "The development of real-time substructure testing," *Philosophical Transactions of the Royal Society of London. Series A: Mathematical, Physical and Engineering Sciences*, vol. 359, no. 1786, pp. 1869-1891, 2001.

- C. Chen and J. M. Ricles, "Large-scale real-time hybrid simulation involving multiple experimental substructures and adaptive actuator delay compensation," *Earthquake Engineering & Structural Dynamics*, vol. 41, no. 3, pp. 549-569, 2012.
- C. Farrar, M. Nishio, F. Hemez, C. Stull, G. Park, P. Cornwell, E. Figueiredo, D.J. Luscher and K. Worden, "Feature Extraction for Structural Dynamics Model Validation," Los Alamos National Lab, Los Alamos, 2016.
- G. A. Fernandois, "Application of model-based compensation methods to real-time hybrid simulation benchmark," *Mechanical Systems and Signal Processing*, vol. 131, pp. 394-416, 2019.
- S. K. Lee, E. C. Park, K. W. Min, S. H. Lee, L. Chung and J. H. Park, "Real-time hybrid shaking table testing method for the performance evaluation of a tuned liquid damper controlling seismic response of building structures," *Journal of Sound and Vibration*, vol. 302, no. 3, pp. 596-612, 2007.
- S. A. Mahin, P. S. B. Shing, C. R. Thewalt and R. D. Hanson, "Pseudodynamic test method—current status and future directions," *Journal of Structural Engineering*, vol. 115, no. 8, pp. 2113-2128, 1989.
- M. Nakashima, H. Kato and E. Takaoka, "Development of real-time pseudo dynamic testing," *Earthquake Engineering & Structural Dynamics*, vol. 21, no. 1, pp. 79-92, 1992.
- D. P. Rohe, " Modal data for the BARC challenge problem Test Report (No. SAND-2018-0640R," *Sandia National Lab.(SNL-NM)*, 2018.
- T. J. Skousen, J. M. Harvie, T. F. Schoenherr, D. Soine and R. Jones, "Designing Hardware for the Boundary Condition Round Robin Challenge (No. SAND2017-11293C)," *Sandia National Lab.(SNL-NM)*, 2017.
- D. E. Soine, R. J. Jones, J. M. Harvie, T. J. Skousen and T. F. Schoenherr, " Designing Hardware for the Boundary Condition Round Robin Challenge," *In Topics in Modal Analysis & Testing*, vol. 9, pp. 119-126, 2019.
- K. Takanashi, K. Udagawa, M. Seki, T. Okada and H. Tanaka, "Nonlinear earthquake response analysis of structures by a computer-actuator on-line system," *Bulletin of Earthquake Resistant Structure Research Center*, vol. 8, pp. 1-17, 1975.
- K. T. H. T. H. Takanashi, "Inelastic response of H-shaped columns to two dimensional earthquake motions," *Bulletin of Earthquake Resistant Structure Research Center*, no. 13, 1980.